Online Appendix: Estimating Macroeconomic News and Surprise Shocks[*]

Lutz Kilian[†] Michael D. Plante[‡] Alexander W. Richter[§]

June 12, 2025

ABSTRACT

Appendix A lists our data sources and transformations. Appendix B proves the existence of an orthogonal rotation matrix in the structural VAR model. Appendices C and D describe in more detail the baseline model and larger-scale DSGE model. Appendix E discusses the identification conditions for the TFP max share estimator. Appendix F discusses the surprise shock max share estimator. Appendix G compares our analysis with the simulation evidence reported in Kurmann and Sims (2021). Appendix H shows empirical max share news estimates for alternative measures of TFP news and alternative vintages of TFP. Appendix I provides additional simulation and estimation results that document the robustness of our findings.

[*]The views expressed in this paper are our own and do not necessarily reflect the views of the Federal Reserve Bank of Dallas or the Federal Reserve System.

[†]Federal Reserve Bank of Dallas, 2200 N Pearl Street, Dallas, TX 75201, and CEPR (lkilian2019@gmail.com).
[‡]Federal Reserve Bank of Dallas, 2200 N Pearl Street, Dallas, TX 75201 (michael.plante@dal.frb.org).
[§]Federal Reserve Bank of Dallas, 2200 N Pearl Street, Dallas, TX 75201 (alex.richter@dal.frb.org).

A DATA SOURCES

We use the following time-series provided by Haver Analytics:

1. **Civilian Noninstitutional Population: 16 Years & Over**
   Not Seasonally Adjusted, Quarterly, Thousands (LN16N@USECON)
2. **Gross Domestic Product: Implicit Price Deflator**
   Seasonally Adjusted, Quarterly, 2012=100 (DGDP@USNA)
3. **Real Gross Domestic Product**
   Seasonally Adjusted, Quarterly, Billions of Chained 2012$ (GDPH@USECON)
4. **Real Personal Consumption Expenditures**
   Seasonally Adjusted, Quarterly, Billions of Chained 2012$ (CH@USECON))
5. **Real Private Fixed Investment**
   Seasonally Adjusted, Quarterly, Billions of Chained 2012$ (FH@USECON)
6. **Hours: Private Sector, Nonfarm Payrolls**
   Seasonally Adjusted, Quarterly, Billions of Hours (LHTPRIVA@USECON)
7. **Fernald Utilization-Adjusted Total Factor Productivity**
   Quarterly, Percent, Annual Rate (TFPMQ@USECON)
8. **Capital Share of Income**, Quarterly (TFPJQ@USECON)
9. **Effective Federal Funds Rate**
   Quarterly Average, Annual Percent (FFED@USECON)
10. **S&P 500 Stock Price Index**, Quarterly Average (SP500@USECON)
11. **Real Research and Development**
    Seasonally Adjusted, Quarterly, Billions of Chained 2012$ (FNPRH@USECON)
12. **Net Stock: Private Fixed Assets**, Annual, Billions of Dollars (EPT@CAPSTOCK)
13. **Net Stock: Durable Goods**, Annual, Billions of Dollars (EDT@CAPSTOCK)
14. **Depreciation: Private Fixed Assets**, Annual, Billions of Dollars (KPT@CAPSTOCK)
15. **Depreciation: Durable Goods**, Annual, Billions of Dollars (KDT@CAPSTOCK)

We also used the following data from other sources:

1. **Information & Communication Technologies Standards Index** from Baron and Schmidt (2019). Data is available at https://www.law.northwestern.edu/research-faculty/clbe/innovationeconomics/data/technologystandards.

2. **Patent-Based Innovation Index** from Cascaldi-Garcia and Vukotić (2022). This is a quarterly version of the Kogan et al. (2017) annual index, which is based on counts of patents where each patent is weighted by its impact on the firm's stock price. Data is available at https://sites.google.com/site/cascaldigarcia/research.

B EXISTENCE OF AN ORTHOGONAL ROTATION MATRIX

Consider the model in Section 2. Observe that either $\gamma_{n,2}\gamma_{n,3} > 0$ and $\gamma_{\ell,2}\gamma_{\ell,3} < 0$ or $\gamma_{n,2}\gamma_{n,3} < 0$ and $\gamma_{\ell,2}\gamma_{\ell,3} > 0$. Using (R1-1) and the solution for γ_s, $\gamma_{\ell,2}$, and $\gamma_{\ell,3}$ in Proposition 1 implies

$$\begin{aligned}
\gamma_{s,1}^2 + \gamma_{s,2}^2 + \gamma_{s,3}^2 &= 1 - \gamma_{n,1}^2 + (\gamma_{n,1}\gamma_{n,2}/\gamma_{s,1})^2 + (\gamma_{n,1}\gamma_{n,3}/\gamma_{s,1})^2 \\
&= 1 - \gamma_{n,1}^2 + (\gamma_{n,1}^2/\gamma_{s,1}^2)(\gamma_{n,2}^2 + \gamma_{n,3}^2) \\
&= 1 \\
\gamma_{\ell,2}^2 + \gamma_{\ell,3}^2 &= 1 - \gamma_{s,2}^2 - \gamma_{n,2}^2 + 1 - \gamma_{s,3}^2 - \gamma_{n,3}^2 \\
&= \gamma_{s,1}^2 + \gamma_{n,1}^2 \\
&= 1 \\
\gamma_{s,1}\gamma_{n,1} + \gamma_{s,2}\gamma_{n,2} + \gamma_{s,3}\gamma_{n,3} &= \gamma_{s,1}\gamma_{n,1} - \gamma_{n,1}\gamma_{n,2}^2/\gamma_{s,1} - \gamma_{n,1}\gamma_{n,3}^2/\gamma_{s,1} \\
&= \gamma_{s,1}\gamma_{n,1} - (\gamma_{n,2}^2 + \gamma_{n,3}^2)\gamma_{n,1}/\gamma_{s,1} \\
&= 0 \\
\gamma_{n,2}\gamma_{\ell,2} + \gamma_{n,3}\gamma_{\ell,3} &= \gamma_{n,2}(\pm\sqrt{1-\gamma_{\ell,3}^2}) + \gamma_{n,3}(\pm\sqrt{1-\gamma_{\ell,2}^2}) \\
&= \gamma_{n,2}(\pm\sqrt{\gamma_{s,3}^2 + \gamma_{n,3}^2}) + \gamma_{n,3}(\pm\sqrt{\gamma_{s,2}^2 + \gamma_{n,2}^2}) \\
&= \gamma_{n,2}(\pm\sqrt{(\gamma_{n,1}^2/\gamma_{s,1}^2 + 1)\gamma_{n,3}^2}) + \gamma_{n,3}(\pm\sqrt{(\gamma_{n,1}^2/\gamma_{s,1}^2 + 1)\gamma_{n,2}^2}) \\
&= \gamma_{n,2}(\pm\sqrt{\gamma_{n,3}^2/\gamma_{s,1}^2}) + \gamma_{n,3}(\pm\sqrt{\gamma_{n,2}^2/\gamma_{s,1}^2}) \\
&= \begin{cases}
\frac{1}{\sqrt{\gamma_{s,1}^2}}\left(\gamma_{n,2}\sqrt{\gamma_{n,3}^2} + \gamma_{n,3}\sqrt{\gamma_{n,2}^2}\right) & \text{if } \gamma_{\ell,2} > 0 \text{ and } \gamma_{\ell,3} > 0 \\
\frac{1}{\sqrt{\gamma_{s,1}^2}}\left(-\gamma_{n,2}\sqrt{\gamma_{n,3}^2} - \gamma_{n,3}\sqrt{\gamma_{n,2}^2}\right) & \text{if } \gamma_{\ell,2} < 0 \text{ and } \gamma_{\ell,3} < 0 \\
\frac{1}{\sqrt{\gamma_{s,1}^2}}\left(-\gamma_{n,2}\sqrt{\gamma_{n,3}^2} + \gamma_{n,3}\sqrt{\gamma_{n,2}^2}\right) & \text{if } \gamma_{\ell,2} < 0 \text{ and } \gamma_{\ell,3} > 0 \\
\frac{1}{\sqrt{\gamma_{s,1}^2}}\left(\gamma_{n,2}\sqrt{\gamma_{n,3}^2} - \gamma_{n,3}\sqrt{\gamma_{n,2}^2}\right) & \text{if } \gamma_{\ell,2} > 0 \text{ and } \gamma_{\ell,3} < 0
\end{cases} \\
&= \begin{cases}
0 & \text{if } \gamma_{n,2}\gamma_{n,3} < 0 \\
0 & \text{if } \gamma_{n,2}\gamma_{n,3} < 0 \\
0 & \text{if } \gamma_{n,2}\gamma_{n,3} > 0 \\
0 & \text{if } \gamma_{n,2}\gamma_{n,3} > 0
\end{cases}
\end{aligned}$$

$$
\begin{aligned}
\gamma_{s,2}\gamma_{\ell,2} + \gamma_{s,3}\gamma_{\ell,3} &= (\gamma_{n,1}/\gamma_{s,1})(\gamma_{n,2}\gamma_{\ell,2} + \gamma_{n,3}\gamma_{\ell,3}) \\
&= 0 \\
\gamma_{s,2}\gamma_{s,3} + \gamma_{n,2}\gamma_{n,3} + \gamma_{\ell,2}\gamma_{\ell,3} &= (\gamma_{n,1}^2/\gamma_{s,1}^2 + 1)\gamma_{n,2}\gamma_{n,3} - (\gamma_{n,2}/\gamma_{n,3})\gamma_{\ell,2}^2 \\
&= \gamma_{n,2}\gamma_{n,3}/\gamma_{s,1}^2 - (\gamma_{n,2}/\gamma_{n,3})(\gamma_{n,3}^2/\gamma_{s,1}^2) \\
&= 0
\end{aligned}
$$

since $\gamma_{s,1}^2 = 1 - \gamma_{n,1}^2 = \gamma_{n,2}^2 + \gamma_{n,3}^2$. Thus, (R1-1)-(R1-6) and (R2-1)-(R2-6) are satisfied, and there exists a Q that is orthogonal.

C BASELINE DSGE MODEL

We detrend the model by scaling trending variables, x_t, as $\tilde{x}_t \equiv x_t/z_t^{1/(1-\alpha)}$, where z_t is the permanent component of TFP. The equilibrium system is given by

$$r_t^k = \alpha mc_t s_t g_t (\tilde{k}_{t-1}/n_t)^{\alpha-1} \tag{C.1}$$
$$\tilde{w}_t = (1-\alpha) mc_t s_t g_t^{-\alpha/(1-\alpha)} (\tilde{k}_{t-1}/n_t)^{\alpha} \tag{C.2}$$
$$\Delta_t^p \tilde{y}_t = s_t g_t^{-\alpha/(1-\alpha)} \tilde{k}_{t-1}^{\alpha} n_t^{1-\alpha} \tag{C.3}$$
$$\tilde{w}_t = \chi n_t^{\eta} \tilde{c}_t \tag{C.4}$$
$$1 = E_t[x_{t+1} r_t/\pi_{t+1}] \tag{C.5}$$
$$\tilde{c}_t + \tilde{\imath}_t = \tilde{y}_t \tag{C.6}$$
$$\tilde{k}_t = (1-\delta)\tilde{k}_{t-1}/g_{y,t} + \mu_t \tilde{\imath}_t \tag{C.7}$$
$$1/\mu_t = E_t[x_{t+1}(r_{t+1}^k + (1-\delta)/\mu_{t+1})] \tag{C.8}$$
$$p_{f,t} = \tfrac{\epsilon_p}{\epsilon_p - 1}(\tilde{f}_{1,t}/\tilde{f}_{2,t}) \tag{C.9}$$
$$\tilde{f}_{1,t} = mc_t \tilde{y}_t + \theta_p E_t[g_{y,t+1} x_{t+1} (\pi_{t+1}/\bar{\pi})^{\epsilon_p} \tilde{f}_{1,t+1}] \tag{C.10}$$
$$\tilde{f}_{2,t} = \tilde{y}_t + \theta_p E_t[g_{y,t+1} x_{t+1} (\pi_{t+1}/\bar{\pi})^{\epsilon_p - 1} \tilde{f}_{2,t+1}] \tag{C.11}$$
$$\Delta_t^p = (1-\theta_p) p_{f,t}^{-\epsilon_p} + \theta_p (\pi_t/\bar{\pi})^{\epsilon_p} \Delta_{t-1}^p \tag{C.12}$$
$$1 = (1-\theta_p) p_{f,t}^{1-\epsilon_p} + \theta_p (\pi_t/\bar{\pi})^{\epsilon_p - 1} \tag{C.13}$$
$$x_t = \beta \tilde{c}_{t-1}/(\tilde{c}_t g_{y,t}) \tag{C.14}$$
$$r_t = \bar{r}(\pi_t/\bar{\pi})^{\phi_\pi} \tag{C.15}$$
$$g_{y,t} = g_t^{1/(1-\alpha)} \tag{C.16}$$
$$\ln s_t = \rho_s \ln s_{t-1} + \sigma_s \varepsilon_{s,t} \tag{C.17}$$
$$\ln g_t = (1-\rho_g)\ln \bar{g} + \rho_g \ln g_{t-1} + \sigma_g \varepsilon_{g,t} \tag{C.18}$$
$$\ln \mu_t = \rho_\mu \ln \mu_{t-1} + \sigma_\mu \varepsilon_{\mu,t} \tag{C.19}$$

Table 1: Baseline DSGE model calibration at quarterly frequency

Parameter	Value	Parameter	Value
Discount Factor (β)	0.995	Steady-State Hours ($\bar{n}$)	0.3333
Cost Share of Capital (α)	0.3343	Steady-State TFP Growth Rate ($\bar{g}$)	1.0026
Capital Depreciation Rate (δ)	0.025	TFP News Shock Persistence (ρ_g)	0.6
Frisch Labor Supply Elasticity ($1/\eta$)	0.5	TFP Surprise Shock Persistence (ρ_s)	0.8
Goods Elasticity of Substitution (ϵ_p)	11	MEI Shock Persistence (ρ_μ)	0.9
Calvo Price Stickiness (θ_p)	0.75	TFP News Shock SD (σ_g)	0.003
Taylor Rule Inflation Response (ϕ_π)	1.5	TFP Surprise Shock SD (σ_s)	0.007
Steady-State Inflation Rate ($\bar{\pi}$)	1.005	MEI Shock SD (σ_μ)	0.007

D LARGER-SCALE DSGE MODEL

We detrend the same way as in the baseline model except $\tilde{\lambda}_t \equiv \lambda_t z_t^{1/(1-\alpha)}$, $\tilde{f}_{1,t}^w \equiv f_{1,t}^w / z_t^{(1+\epsilon_w)/(1-\alpha)}$, and $\tilde{f}_{2,t}^w \equiv f_{2,t}^w / z_t^{\epsilon_w/(1-\alpha)}$. The labor share $\omega_{\ell,t} = w_{\ell,t} l_{s,t}/y_t$. The equilibrium system is given by

$$r_{k,t} = \alpha mc_t s_t (\tilde{k}_{s,t}/l_{s,t})^{\alpha-1} \tag{D.1}$$

$$\tilde{w}_{\ell,t} = (1-\alpha) mc_t s_t (\tilde{k}_{s,t}/l_{s,t})^{\alpha} \tag{D.2}$$

$$\Delta_t^p \tilde{y}_t = s_t \tilde{k}_{s,t}^{\alpha} l_{s,t}^{1-\alpha} - \bar{F} \tag{D.3}$$

$$\tilde{\lambda}_t = (\tilde{c}_t - b\tilde{c}_{t-1}/g_{y,t})^{-1} - \beta b E_t[(\tilde{c}_{t+1} g_{y,t+1} - b\tilde{c}_t)^{-1}] \tag{D.4}$$

$$1 = E_t[x_{t+1} r_t / \pi_{t+1}] \tag{D.5}$$

$$r_{k,t} = \gamma_1 + \gamma_2 (u_t - 1) \tag{D.6}$$

$$\theta \kappa_3 e_t^{\kappa_4 - 1} = \tilde{\lambda}_t \tilde{w}_t h_t \tag{D.7}$$

$$\theta \kappa_1 h_t^{\kappa_2 - 1} = \tilde{\lambda}_t \tilde{w}_t e_t \tag{D.8}$$

$$\begin{aligned} &\theta(\kappa_0 + (\kappa_1/\kappa_2) h_t^{\kappa_2} + (\kappa_3/\kappa_4) e_t^{\kappa_4}) \\ &= \tilde{\lambda}_t \tilde{w}_t \left[e_t h_t - \tfrac{\psi}{2}(n_t/n_{t-1} - 1)^2 - \psi(n_t/n_{t-1} - 1)(n_t/n_{t-1})\right] \\ &\quad + \beta\psi E_t[\tilde{\lambda}_{t+1} \tilde{w}_{t+1} (n_{t+1}/n_t - 1)(n_{t+1}/n_t)^2] \end{aligned} \tag{D.9}$$

$$\tilde{k}_t = (1-\delta)\tilde{k}_{t-1}/g_{y,t} + \mu_t \tilde{\imath}_t \tag{D.10}$$

$$\mu_t q_t = 1 + \varphi(\Phi_t - \tilde{\delta}) \tag{D.11}$$

$$\begin{aligned} q_t = E_t[x_{t+1}(&r_{k,t+1} u_{t+1} - \gamma_1(u_{t+1} - 1) - \tfrac{\gamma_2}{2}(u_{t+1} - 1)^2 \\ &- \tfrac{\varphi}{2}(\Phi_{t+1} - \tilde{\delta})^2 + \varphi(\Phi_{t+1} - \tilde{\delta})\Phi_{t+1} + (1-\delta) q_{t+1})] \end{aligned} \tag{D.12}$$

$$\Phi_t = \tilde{\imath}_t g_{y,t} / \tilde{k}_{t-1} \tag{D.13}$$

$$l_t = e_t h_t n_t \tag{D.14}$$

$$l_t = \Delta_t^w l_{s,t} \tag{D.15}$$

$$\tilde{k}_{s,t} = u_t \tilde{k}_{t-1}/g_{y,t} \tag{D.16}$$

$$x_t = \beta\tilde{\lambda}_t/(\tilde{\lambda}_{t-1}g_{y,t}) \tag{D.17}$$

$$\tilde{p}_t = \tfrac{\epsilon_p}{\epsilon_p-1}(\tilde{f}^p_{1,t}/\tilde{f}^p_{2,t}) \tag{D.18}$$

$$\tilde{f}^p_{1,t} = mc_t\tilde{y}_t + \theta_p E_t[x_{t+1}\pi_t^{-\epsilon_p\gamma_p}\bar{\pi}^{-\epsilon_p(1-\gamma_p)}\pi_{t+1}^{\epsilon_p}\tilde{f}^p_{1,t+1}g_{y,t+1}] \tag{D.19}$$

$$\tilde{f}^p_{2,t} = \tilde{y}_t + \theta_p E_t[x_{t+1}\pi_t^{(1-\epsilon_p)\gamma_p}\bar{\pi}^{(1-\epsilon_p)(1-\gamma_p)}\pi_{t+1}^{\epsilon_p-1}\tilde{f}^p_{2,t+1}g_{y,t+1}] \tag{D.20}$$

$$\Delta^p_t = (1-\theta_p)\tilde{p}_t^{-\epsilon_p} + \theta_p\pi_{t-1}^{-\epsilon_p\gamma_p}\bar{\pi}^{-\epsilon_p(1-\gamma_p)}\pi_t^{\epsilon_p}\Delta^p_{t-1} \tag{D.21}$$

$$1 = (1-\theta_p)\tilde{p}_t^{1-\epsilon_p} + \theta_p\pi_{t-1}^{(1-\epsilon_p)\gamma_p}\bar{\pi}^{(1-\epsilon_p)(1-\gamma_p)}\pi_t^{\epsilon_p-1} \tag{D.22}$$

$$\tilde{w}^*_{\ell,t} = \tfrac{\epsilon_w}{\epsilon_w-1}(\tilde{f}^w_{1,t}/\tilde{f}^w_{2,t}), \tag{D.23}$$

$$\tilde{f}^w_{1,t} = \tilde{w}^{\epsilon_w}_{\ell,t}\tilde{w}_t l_{s,t} + \theta_w\bar{g}_y E_t[x_{t+1}\pi_{t+1}^{\epsilon_w}\pi_t^{-\epsilon_w\gamma_w}\bar{\pi}^{-\epsilon_w(1-\gamma_w)}\tilde{f}^w_{1,t+1}(g_{y,t+1}/\bar{g}_y)^{1+\epsilon_w}] \tag{D.24}$$

$$\tilde{f}^w_{2,t} = \tilde{w}^{\epsilon_w}_{\ell,t}l_{s,t} + \theta_w\bar{g}_y E_t[x_{t+1}\pi_{t+1}^{\epsilon_w-1}\pi_t^{(1-\epsilon_w)\gamma_w}\bar{\pi}^{(1-\epsilon_w)(1-\gamma_w)}\tilde{f}^w_{2,t+1}(g_{y,t+1}/\bar{g}_y)^{\epsilon_w}] \tag{D.25}$$

$$\Delta^w_t = (1-\theta_w)\left(\frac{\tilde{w}^*_{\ell,t}}{\tilde{w}_{\ell,t}}\right)^{-\epsilon_w} + \theta_w\pi_{t-1}^{-\epsilon_w\gamma_w}\bar{\pi}^{-\epsilon_w(1-\gamma_w)}\pi_t^{\epsilon_w}\left(\frac{\tilde{w}_{\ell,t-1}\bar{g}_y}{\tilde{w}_{\ell,t}g_{y,t}}\right)^{-\epsilon_w}\Delta^w_{t-1} \tag{D.26}$$

$$\tilde{w}^{1-\epsilon_w}_{\ell,t} = (1-\theta_w)(\tilde{w}^*_{\ell,t})^{1-\epsilon_w} + \theta_w\pi_{t-1}^{\gamma_w(1-\epsilon_w)}\bar{\pi}^{(1-\gamma_w)(1-\epsilon_w)}\pi_t^{\epsilon_w-1}\left(\frac{\tilde{w}_{\ell,t-1}\bar{g}_y}{g_{y,t}}\right)^{1-\epsilon_w} \tag{D.27}$$

$$r_t = r_{t-1}^{\rho_r}(\bar{r}(\pi_t/\bar{\pi})^{\phi_\pi}(\tilde{y}_t g_{y,t}/(\tilde{y}_{t-1}\bar{g}_y))^{\phi_y})^{1-\rho_r}\exp(\sigma_r\varepsilon_{r,t}) \tag{D.28}$$

$$\begin{aligned}\tilde{c}_t + \tilde{\imath}_t + \tfrac{\psi}{2}(n_t/n_{t-1}-1)^2\tilde{w}_t n_t + \tfrac{\varphi}{2}(\Phi_t-\bar{\delta})^2\tilde{k}_{t-1}/g_{y,t}\\ +(\gamma_1(u_t-1)+\tfrac{\gamma_2}{2}(u_t-1)^2)\tilde{k}_{t-1}/g_{y,t} = \tilde{y}_t\end{aligned} \tag{D.29}$$

$$g_{y,t} = g_t^{1/(1-\alpha)} \tag{D.30}$$

$$\ln s_t = \rho_s \ln s_{t-1} + \sigma_s\varepsilon_{s,t} \tag{D.31}$$

$$\ln g_t = (1-\rho_g)\ln g + \rho_g\ln g_{t-1} + \sigma_g\varepsilon_{g,t} \tag{D.32}$$

$$\ln \mu_t = \rho_\mu \ln\mu_{t-1} + \sigma_\mu\varepsilon_{\mu,t} \tag{D.33}$$

E IDENTIFICATION CONDITIONS

As long as TFP innovations are fully explained by news and surprise shocks, as would be the case in the absence of TFP measurement error, it has to be the case that $\gamma_{\ell,1} = 0$. Whether one imposes this restriction does not affect the estimate of the news shock, but it determines whether the surprise shock can also be identified. To formalize this result, assume $\gamma_{\ell,1} = 0$, and note that the Q matrix is orthogonal if and only if $Q'Q = QQ' = I_3$. This yields the restrictions

$$\begin{pmatrix}\gamma_{s,1} & \gamma_{s,2} & \gamma_{s,3}\\ \gamma_{n,1} & \gamma_{n,2} & \gamma_{n,3}\\ 0 & \gamma_{\ell,2} & \gamma_{\ell,3}\end{pmatrix}\begin{pmatrix}\gamma_{s,1} & \gamma_{n,1} & 0\\ \gamma_{s,2} & \gamma_{n,2} & \gamma_{\ell,2}\\ \gamma_{s,3} & \gamma_{n,3} & \gamma_{\ell,3}\end{pmatrix} = \begin{pmatrix}1 & 0 & 0\\ 0 & 1 & 0\\ 0 & 0 & 1\end{pmatrix}, \tag{R1}$$

Table 2: Larger-scale DSGE model parameterization at quarterly frequency

Parameter	Value	Parameter	Value
Discount Factor (β)	0.99	Taylor Rule Inflation Response (ϕ_π)	1.5
Cost Share of Capital (α)	0.3333	Taylor Rule Output Response (ϕ_y)	0.5
Capital Depreciation Rate (δ)	0.025	Taylor Rule Smoothing (ρ_r)	0.8
Utilization Function Curvature (γ_2)	0.01	Steady-State Inflation Rate ($\bar{\pi}$)	1
Internal Habit Persistence (b)	0.8	Steady-State Employment Share ($\bar{n}$)	3/5
Capital Adjustment Cost (φ)	2	Steady-State Labor Preference ($\bar{G}$)	1/3
Employment Adjustment Cost (ψ)	2	Steady-State Effort ($\bar{e}$)	5
Frisch Elasticity of Hours (η)	1	Steady-State Hours ($\bar{h}$)	1/3
Elasticity of Effort to Hours (ϵ_{eh})	4	Steady-State Output Growth Rate ($\bar{g}_y$)	1.0026
Goods Elasticity of Substitution (ϵ_p)	11	TFP News Shock Persistence (ρ_g)	0.7
Labor Elasticity of Substitution (ϵ_w)	11	TFP Surprise Shock Persistence (ρ_s)	0.9
Calvo Price Stickiness (θ_p)	0.75	MEI Shock Persistence (ρ_μ)	0.8
Calvo Wage Stickiness (θ_w)	0.9	TFP News Shock SD (σ_g)	0.002125
Price Indexation (γ_p)	0	TFP Surprise Shock SD (σ_s)	0.000425
Wage Indexation (γ_w)	1	MEI Shock SD (σ_μ)	0.00425

$$\begin{pmatrix} \gamma_{s,1} & \gamma_{n,1} & 0 \\ \gamma_{s,2} & \gamma_{n,2} & \gamma_{\ell,2} \\ \gamma_{s,3} & \gamma_{n,3} & \gamma_{\ell,3} \end{pmatrix} \begin{pmatrix} \gamma_{s,1} & \gamma_{s,2} & \gamma_{s,3} \\ \gamma_{n,1} & \gamma_{n,2} & \gamma_{n,3} \\ 0 & \gamma_{\ell,2} & \gamma_{\ell,3} \end{pmatrix} = \begin{pmatrix} 1 & 0 & 0 \\ 0 & 1 & 0 \\ 0 & 0 & 1 \end{pmatrix}. \tag{R2}$$

Restriction R1 implies

$$\gamma_{n,1}^2 + \gamma_{n,2}^2 + \gamma_{n,3}^2 = 1, \tag{R1-1}$$

$$\gamma_{s,2}\gamma_{\ell,2} + \gamma_{s,3}\gamma_{\ell,3} = 0, \tag{R1-2}$$

$$\gamma_{n,2}\gamma_{\ell,2} + \gamma_{n,3}\gamma_{\ell,3} = 0, \tag{R1-3}$$

$$\gamma_{s,1}^2 + \gamma_{s,2}^2 + \gamma_{s,3}^2 = 1, \tag{R1-4}$$

$$\gamma_{\ell,2}^2 + \gamma_{\ell,3}^2 = 1, \tag{R1-5}$$

$$\gamma_{s,1}\gamma_{n,1} + \gamma_{s,2}\gamma_{n,2} + \gamma_{s,3}\gamma_{n,3} = 0. \tag{R1-6}$$

Restriction R2 implies

$$\gamma_{s,1}^2 + \gamma_{n,1}^2 = 1, \tag{R2-1}$$

$$\gamma_{s,1}\gamma_{s,2} + \gamma_{n,1}\gamma_{n,2} = 0, \tag{R2-2}$$

$$\gamma_{s,1}\gamma_{s,3} + \gamma_{n,1}\gamma_{n,3} = 0, \tag{R2-3}$$

$$\gamma_{s,2}^2 + \gamma_{n,2}^2 + \gamma_{\ell,2}^2 = 1, \tag{R2-4}$$

$$\gamma_{s,3}^2 + \gamma_{n,3}^2 + \gamma_{\ell,3}^2 = 1, \tag{R2-5}$$

$$\gamma_{s,2}\gamma_{s,3} + \gamma_{n,2}\gamma_{n,3} + \gamma_{\ell,2}\gamma_{\ell,3} = 0. \tag{R2-6}$$

An estimate of γ_n is obtained by maximizing the forecast error variance share of the news shock subject to (R1-1). Given γ_n, (R2-1)-(R2-5) imply

$$\gamma_{s,1} = \pm\sqrt{1-\gamma_{n,1}^2}, \quad \gamma_{s,2} = -\frac{\gamma_{n,1}\gamma_{n,2}}{\gamma_{s,1}}, \quad \gamma_{s,3} = -\frac{\gamma_{n,1}\gamma_{n,3}}{\gamma_{s,1}},$$
$$\gamma_{\ell,2} = \pm\sqrt{1-\gamma_{s,2}^2-\gamma_{n,2}^2}, \quad \gamma_{\ell,3} = \pm\sqrt{1-\gamma_{s,3}^2-\gamma_{n,3}^2}.$$

Thus, for $K = 3$ the identifying restrictions uniquely pin down all three structural response functions up to their sign. This means that all that is required to recover the news and surprise shocks is a normalizing assumption to the effect that the surprise shock has a positive impact effect on TFP and the news shock has a positive effect on TFP at H_n. For $K > 3$ only the news and surprise shocks can be recovered.

While our example is for $K = 3$, the following proposition shows that without TFP measurement error the TFP max share estimator of the news shock always identifies the surprise shock.

Proposition 1. *In the absence of TFP measurement error, γ_s will be uniquely determined for any given estimate of γ_n obtained using the TFP max share estimator. In particular, when TFP is ordered first in the VAR model, $\gamma_{s,1} = \pm\sqrt{1-\gamma_{n,1}^2}$ and $\gamma_{s,j} = -\gamma_{n,1}\gamma_{n,j}/\gamma_{s,1}$ for $j \in \{2,\ldots,K\}$.*

The proof immediately follows from a generalization of the analysis for $K = 3$. Note that there are multiple solutions for Q, some of which will satisfy R1 and R2 and some of which may not. For $K = 3$, for example, there are 2^3 possible solutions. The validity of the estimator requires the existence of an orthogonal Q matrix. In Appendix B, we showed that when solving for γ_n and γ_s, γ_ℓ can always be chosen such that Q is orthogonal. This result generalizes to $K > 3$.

Our analysis highlights that the TFP max share estimator will be able to deliver estimates of the surprise shock even when there is no restriction on $\gamma_{n,1}$, as long as there is no TFP measurement error. This allows us to shed light on the ability of the TFP max share estimator to recover the population responses to news and surprise shocks under ideal conditions without TFP measurement error. If the estimator does not work in this setting, it would not be expected to work in the more realistic setting when TFP has to be recovered from the observed data by removing the estimated factor utilization, creating TFP measurement error.

F SURPRISE SHOCK MAX SHARE ESTIMATOR

An implication of our analysis in Appendix E is that we can either estimate γ_s given an estimate of γ_n obtained by maximizing the TFP forecast error variance share at a long horizon or, alternatively, we can estimate γ_n given an estimate of γ_s obtained by maximizing the TFP forecast error variance share at a short horizon. In other words, the estimator of γ_n is not unique. This raises the question of which estimator should be used when there is no TFP measurement error. A surprise shock max

Figure 1: Impulse responses from alternative estimators based on the baseline DSGE model

(a) News shock

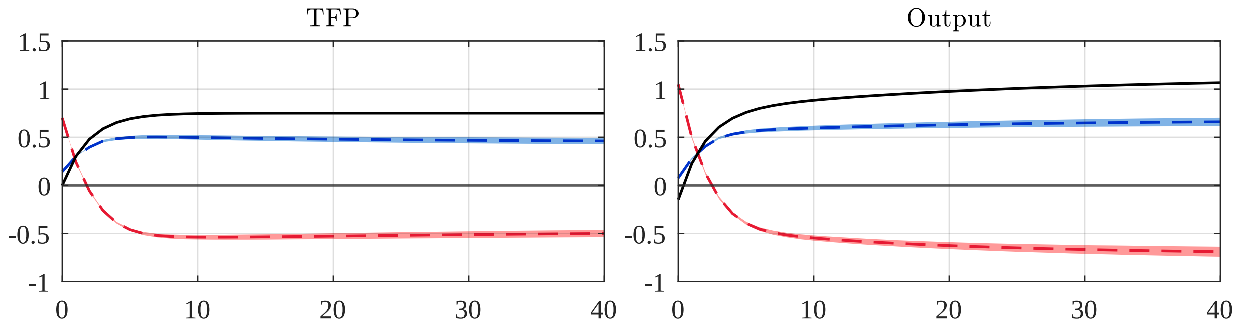

(b) Surprise shock

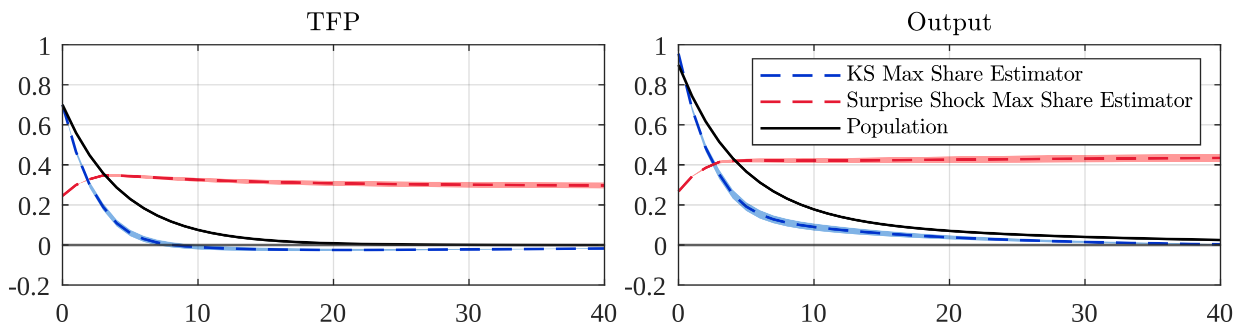

Notes: VAR(4) model with $T = 10{,}000$ and $\mathbf{y}_t = (a_t, y_t, i_t)'$.

share estimator can be defined as

$$\gamma_s = \text{argmax } \Omega_{1,1}(H_s), \quad \Omega_{1,1}(H_s) \equiv \frac{\sum_{\tau=0}^{H_s} \Phi_{1,\tau} P \gamma_s \gamma_s' P' \Phi_{1,\tau}'}{\sum_{\tau=0}^{H_s} \Phi_{1,\tau} \Sigma \Phi_{1,\tau}'},$$

subject to the restriction that $\gamma_s'\gamma_s = 1$ and that the responses of selected variables to the surprise shock match patterns that would be expected of a surprise shock, where $\gamma_s = (\gamma_{s,1}, \gamma_{s,2}, \gamma_{s,3})'$ denotes the first column in the orthogonal rotation matrix Q and the horizon H_s is set to four quarters. Similarly inaccurate results are obtained for shorter horizons.

Figure 1 shows that not only is the surprise shock max share estimator much more biased than the original estimator, but it also tends to generate impulse responses that are increasing when the population response is declining and that are declining when the population response is increasing. In fact, responses to these surprise shocks look much like one would expect responses to a news shock to look like. Moreover, the responses to the news shock are of the opposite sign of the population responses. Thus, this alternative estimator should not be used in applied work.

G Comparison with Kurmann-Sims Simulation Evidence

Table 3: Data and model-implied moments under Kurmann and Sims (2021) TFP parameters

(a) Baseline model

Moment	Data	Model	Moment	Data	Model
$SD(\tilde{a}_t)$	2.01	1.46	$SD(\tilde{\imath}_t)$	9.63	7.47
$SD(\Delta a_t)$	0.80	0.30	$AC(\tilde{a}_t)$	0.87	0.88
$SD(\tilde{y}_t)$	3.13	1.88	$AC(\Delta a_t)$	−0.09	0.67

(b) Larger-scale model

Moment	Data	Model	Moment	Data	Model
$SD(\tilde{a}_t)$	2.01	2.67	$SD(\tilde{\imath}_t)$	9.63	12.15
$SD(\Delta a_t)$	0.80	0.59	$AC(\tilde{a}_t)$	0.87	0.88
$SD(\tilde{y}_t)$	3.13	5.15	$AC(\Delta a_t)$	−0.09	0.43

Notes: A tilde denotes a detrended variable and Δ is a log change. In the data, a_t is Fernald utilization-adjusted TFP. For the baseline model, actual and measured TFP coincide. For the larger-scale model, a_t, is measured TFP (TFP_t^u).

Contrary to our findings, Kurmann and Sims (2021) report having some success identifying the news shock in a Monte Carlo exercise with $T = 10{,}000$ based on a larger-scale DSGE model. The key difference is not the structure of the model, but that they use a different parameterization for the TFP process ($\rho_g = 0.7$, $\rho_s = 0.9$, $\sigma_g = 0.002125$ and $\sigma_s = 0.000425$). They note that their TFP parameterization is based on standard values in the literature. However, most DSGE models feature either a stationary or permanent TFP shock process. When a model features both processes, standard values from models with only one process can lead to TFP moments that are at odds with actual data. The most notable difference from our calibration is that the standard deviation of their surprise shock is only about 6% of our baseline value.

Table 3a reports simulated moments when using the Kurmann and Sims (2021) parameterization of the TFP process in our baseline model. These results show that their specification is at odds with the data. In particular, the autocorrelation of TFP growth is quite high in the model but close to zero in the data. Table 3b shows that this continues to be the case even when we use the larger-scale DSGE model and allow for TFP measurement error. While the 0.43 autocorrelation of the growth rate of measured TFP is lower than what is reported in the baseline model, it remains well above the data.

The unrealistically high persistence of the TFP growth process under the Kurmann and Sims (2021) parameterization is important for understanding their findings because it drives the forecast error variance decomposition of TFP in the DSGE model. As shown in Table 4, the news shock

Table 4: Forecast error variance decompositions under Kurmann and Sims (2021) TFP parameters

(a) Baseline model, true TFP ($\ln a_t$)

	Horizon				
Shock	4	8	20	40	80
News	98.6	99.6	99.9	99.9	100.0
Surprise	1.4	0.4	0.1	0.1	0.0
MEI	0.0	0.0	0.0	0.0	0.0

(b) Larger-scale model, true TFP ($\ln a_t$)

	Horizon				
Shock	4	8	20	40	80
News	98.6	99.6	99.9	99.9	100.0
Surprise	1.4	0.4	0.1	0.1	0.0
MEI	0.0	0.0	0.0	0.0	0.0

(c) Larger-scale model, measured TFP ($\ln \mathrm{TFP}_t^u$)

	Horizon				
Shock	4	8	20	40	80
News	72.1	79.1	52.6	84.0	94.5
Surprise	1.0	0.6	0.4	0.3	0.1
MEI	27.0	20.3	47.0	15.8	5.4

Notes: MEI denotes marginal efficiency of investment.

explains the vast majority of the variance at all horizons when using the Kurmann-Sims parameterization in the baseline model and in the larger-scale DSGE model. Thus, their parameterization effectively eliminates the surprise shock and makes it much easier for the KS estimator to identify the news shock. This explains the comparatively high accuracy of the KS estimator in their simulation analysis.

Figure 2 plots the responses of output and measured TFP under the Kurmann-Sims parameterization of the larger-scale DSGE model for $T = 10{,}000$. The top panel shows the results in the absence of measurement error. As expected, the KS estimator does an excellent job at recovering the population responses when the sample size is sufficiently large. The bottom panel shows the results with measurement error. While the bias of the output response is slightly larger, the fit remains quite good. There is a discrepancy between the response of measured TFP to a news shock and the population response of true TFP, which is also apparent in the simulation evidence reported in Kurmann and Sims (2021). However, this result is not surprising. With measurement

Figure 2: KS estimator of responses to a news shock under the Kurmann-Sims parameterization

(a) Larger-scale model without measurement error

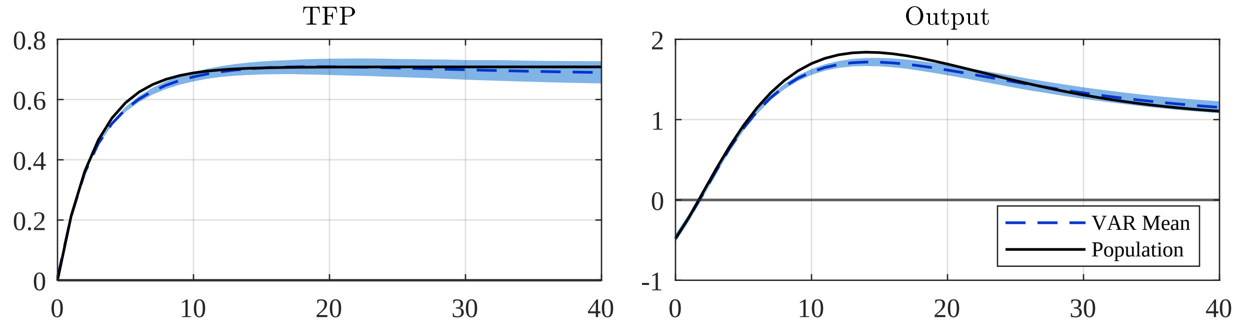

(b) Larger-scale with measurement error

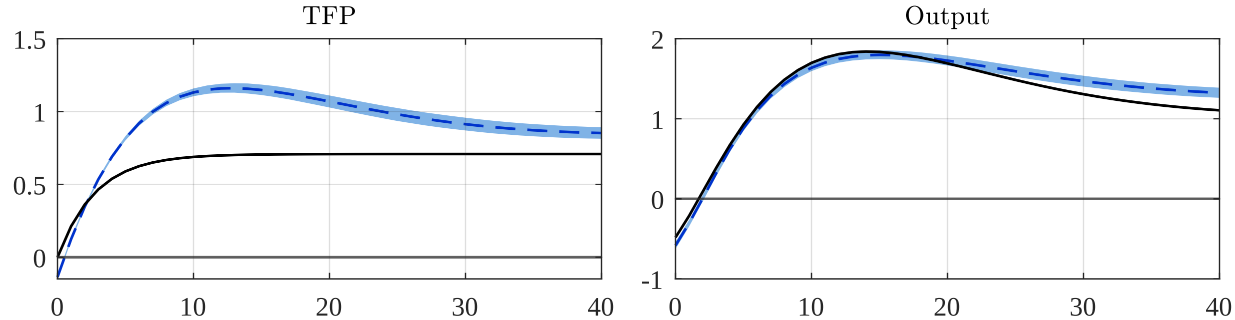

Notes: Based on a VAR(4) model with $T = 10{,}000$ for $\mathbf{y}_t = (a_t, y_t, i_t)'$ when there is no measurement error and $\mathbf{y}_t = (\text{TFP}_t^u, y_t, i_t)'$ where there is measurement error.

Table 5: RMSE over 40 quarters under the Kurmann-Sims parameterization

Estimator	TFP Response	Output Response	Investment Response	Total
KS Max Share	11.3	4.9	7.6	23.8
NAMS	10.9	4.3	5.9	21.1
Max Share News	8.8	2.6	5.0	16.4
Alt KS Max Share	9.0	3.1	6.6	18.7
Alt NAMS	8.6	3.0	6.3	17.9

Notes: VAR(4) model with $T = 10{,}000$, where $\mathbf{y}_t = (\text{TFP}_t^u, y_t, i_t)$ for the KS max share estimator and $\mathbf{y}_t = (z_{t+1}, \text{TFP}_t^u, y_t, i_t)$ for the max share news estimator. The Alt KS max share estimator uses the KS identification strategy and the max share news model variables. The Alt NAMS estimator uses the NAMS identification strategy and the max share news model variables.

error there is no reason to expect the VAR to recover the TFP response, since the VAR is estimated with measured TFP and the population response is based on true TFP.

Finally, it should be noted that, even under the KS parameterization of TFP, the KS max share and NAMS estimators are outperformed by the Alt KS max share and Alt NAMS estimators, respectively, which in turn are less accurate than the max share news estimator (see Table 5).

H Additional Empirical Results

This section shows the responses from 9-variable VAR models with alternative TFP news series (Figure 3) and responses from a 4-variable VAR model with different vintages of TFP (Figure 4).

Figure 3: Max share news estimates for alternative measures of TFP news

(a) R&D expenditures

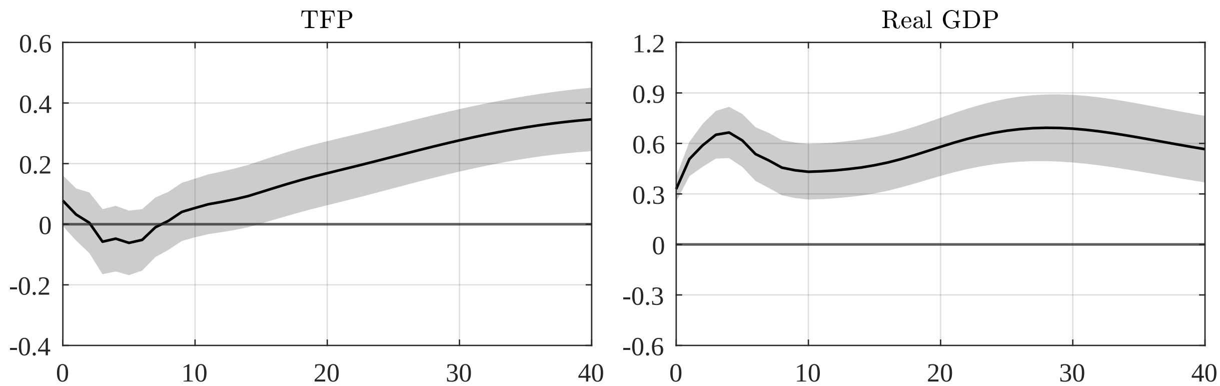

(b) ICT index

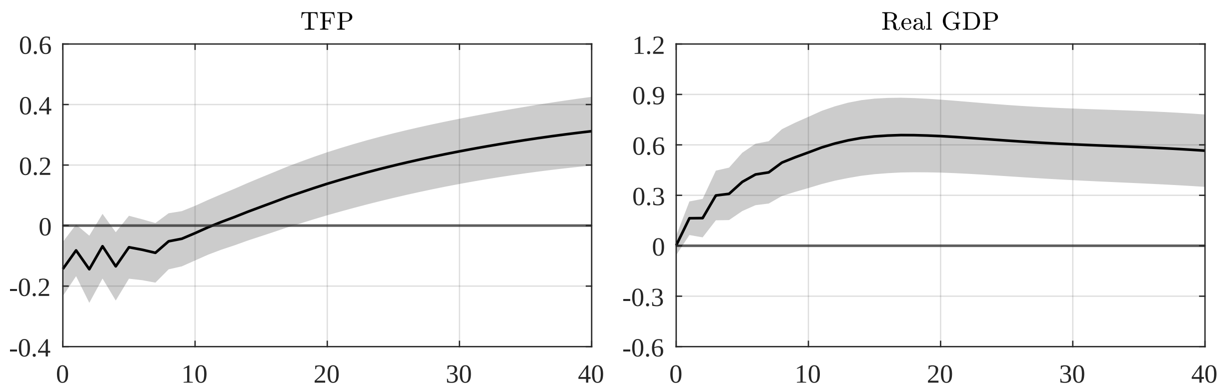

(c) CGV series

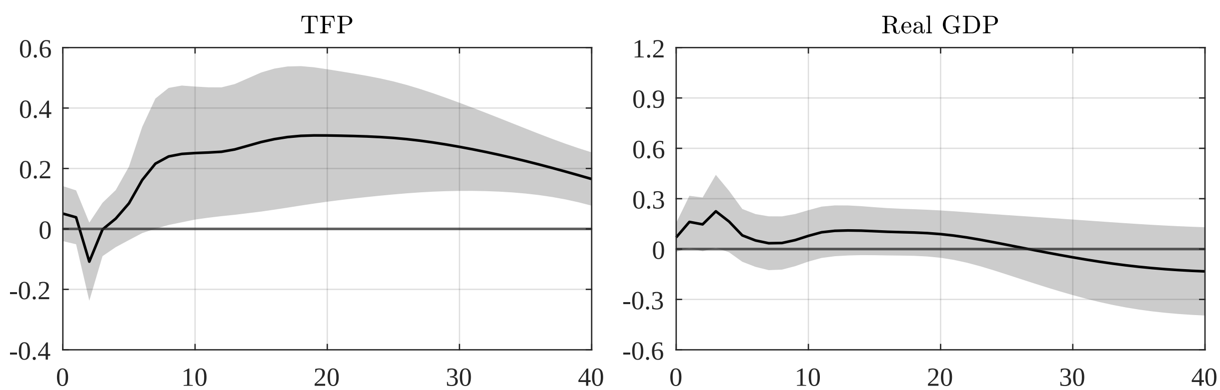

Notes: VAR(4) models estimated on identical samples from 1960-2010 using the 9-variable VAR model. Shaded regions represent 1-standard deviation error bands computed by residual-based bootstrap for the max share news estimator. Responses are in percent deviations from the baseline.

Figure 4: Impulse responses to a news shock with different vintages of TFP

(a) BS max share estimator

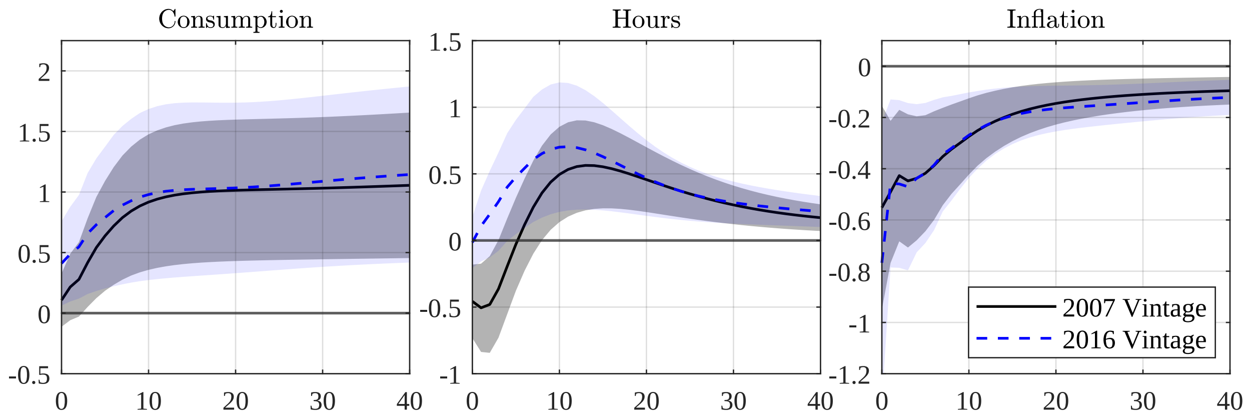

(b) KS max share estimator

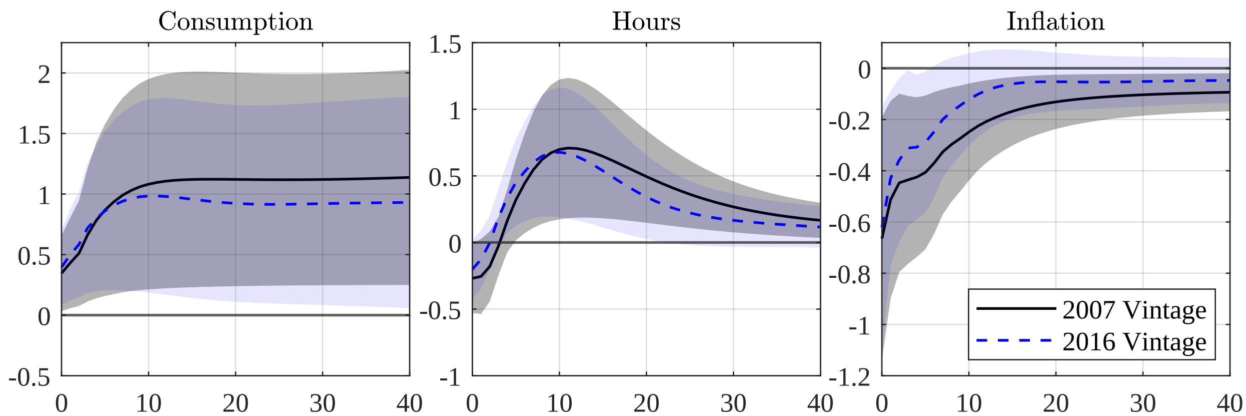

(c) Max share news estimator

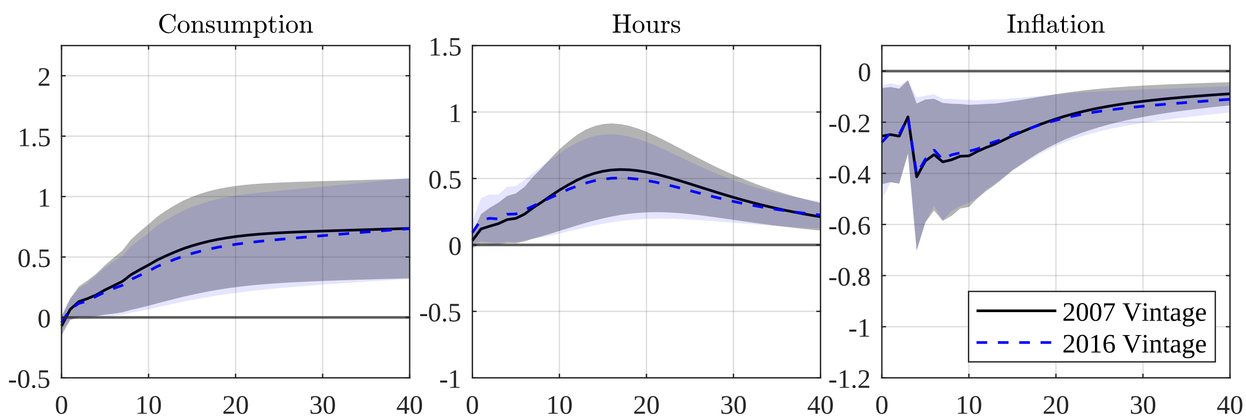

Notes: The BS and KS max share estimators are based on a VAR(4) model with log TFP, log consumption, log hours, and inflation. The model for the max share news estimator also includes the ICT index. The sample is 1960Q1 to 2007Q4. The vintages match those in Figure 1 of Kurmann and Sims (2021). The data for TFP, consumption, hours, and inflation come from the replication package of Kurmann and Sims (2021). Shaded regions represent 1-standard deviation error bands computed by residual-based bootstrap. Responses are in percent deviations from the baseline.

I Additional Robustness Checks

This section presents several additional results:

- RMSEs of alternative estimators based on the larger-scale DSGE model with the news shock occurring with a delay of $k \in \{0, 1, 2, 4\}$ quarters (Table 6).
- RMSEs of alternative estimators with five variables in the VAR model and five shocks in the larger-scale DSGE model (Table 7).
- Impulse responses based on max share estimators that target labor productivity (Figure 5).
- RMSEs of alternative max share estimators that target output (Table 8).
- Results under alternative calibrations of the larger-scale DSGE model (parameters, Table 9; model fit, Table 10; FEVD, Table 11; RMSE of alternative estimators, Table 12).

Table 6: RMSE over 40 quarters based on the larger-scale DSGE model with different news lags

(a) KS max share estimator

News Shock	TFP	Output	Investment	Total
No Lags ($\varepsilon_{g,t}$)	10.1	11.2	20.7	42.1
1 Lag ($\varepsilon_{g,t-1}$)	10.3	10.4	19.3	40.0
2 Lags ($\varepsilon_{g,t-2}$)	10.4	9.4	17.5	37.2
4 Lags ($\varepsilon_{g,t-4}$)	10.8	7.4	14.3	32.5

(b) NAMS estimator

News Shock	TFP	Output	Investment	Total
No Lags ($\varepsilon_{g,t}$)	10.0	11.6	23.0	44.6
1 Lag ($\varepsilon_{g,t-1}$)	10.1	10.8	21.3	42.2
2 Lags ($\varepsilon_{g,t-2}$)	10.3	9.7	19.1	39.0
4 Lags ($\varepsilon_{g,t-4}$)	10.8	7.4	14.2	32.4

(c) Max share news estimator

News Shock	TFP	Output	Investment	Total
No Lags ($\varepsilon_{g,t}$)	6.1	2.9	8.1	17.2
1 Lag ($\varepsilon_{g,t-1}$)	6.4	2.8	7.6	16.7
2 Lags ($\varepsilon_{g,t-2}$)	6.9	2.6	7.1	16.6
4 Lags ($\varepsilon_{g,t-4}$)	8.1	2.4	6.5	16.9

Notes: Results based on $T = 10{,}000$. The VAR includes $\mathbf{y}_t = (\mathrm{TFP}^u_t, y_t, i_t)'$ for the KS max share and NAMS estimators and $\mathbf{y}_t = (z_{t+k}, \mathrm{TFP}^u_t, y_t, i_t)$ for the max share news estimator with k lags.

Table 7: RMSE over 40 quarters based on the larger-scale DSGE model with five shocks

Estimator	TFP	Output	Investment	Consumption	Labor	Total
KS Max Share	7.3	4.5	18.8	2.9	4.4	37.9
BS Max Share	7.3	3.8	17.1	2.9	3.9	35.0
NAMS	6.8	4.5	16.4	2.1	3.7	33.6
Max Share News	6.1	2.7	8.2	1.5	2.3	20.8

Notes: VAR(4) model with $T = 10{,}000$. $\mathbf{y}_t = (\text{TFP}_t^u, y_t, i_t, c_t, l_t)$ for the TFP max share estimators and $\mathbf{y}_t = (z_{t+1}^n, \text{TFP}_t^u, y_t, i_t, c_t, l_t)'$ for the max share news estimator.

Figure 5: Impulse responses to a news shock when targeting labor productivity

(a) KS max share estimator

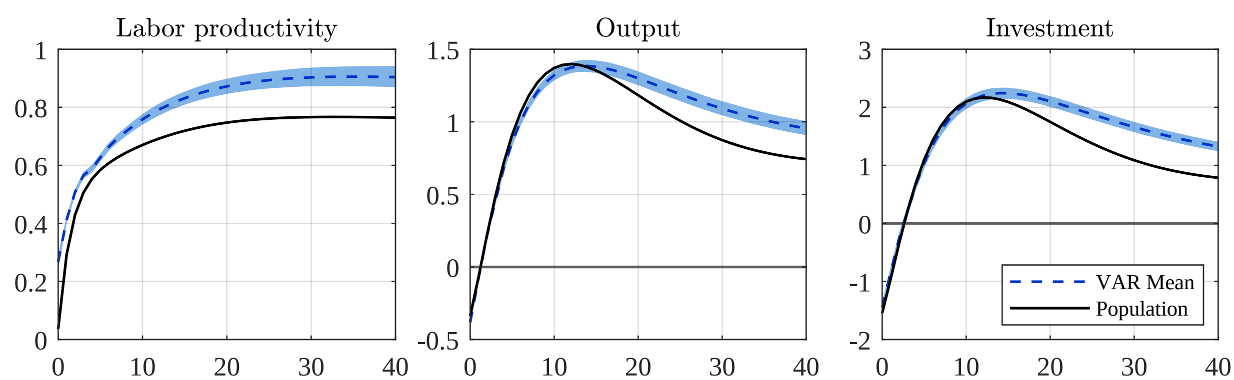

(b) NAMS estimator

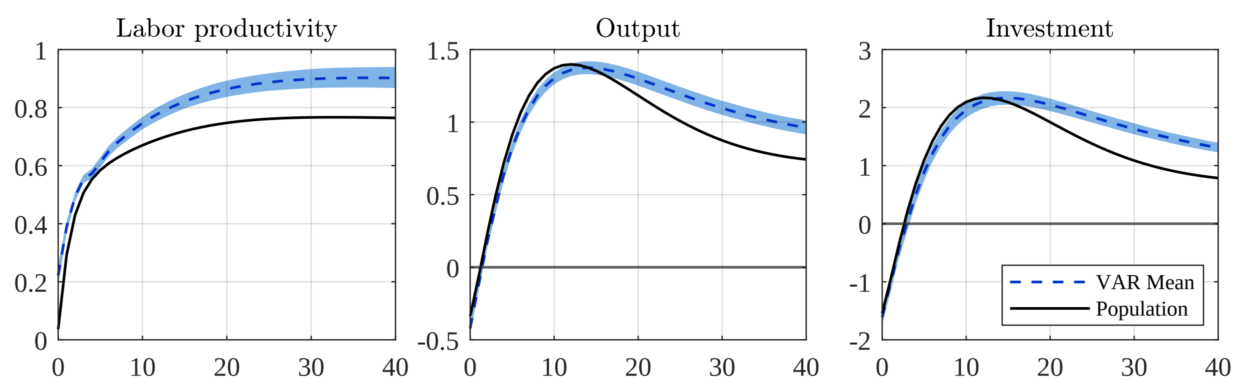

Notes: Based on the larger-scale DSGE model. VAR(4) model with $T = 10{,}000$ and $\mathbf{y}_t = (lp_t, y_t, i_t)$, where lp_t is labor productivity.

Table 8: RMSE over 40 quarters when targeting output compared to max share news estimator

Estimator	TFP	Output	Investment	Total
Max Share Output	9.7	9.5	15.7	35.0
NAMS Output	10.2	10.5	19.7	40.4
Max Share News	6.4	2.8	7.6	16.8

Notes: Based on the larger-scale DSGE model. VAR(4) model with $T = 10{,}000$. $\mathbf{y}_t = (\text{TFP}_t^u, y_t, i_t)$ for the TFP max share estimators and $\mathbf{y}_t = (z_{t+1}, \text{TFP}_t^u, y_t, i_t)$ for the max share news estimator.

Table 9: Parameters for alternative larger-scale DSGE models

Parameter	Baseline	Alternative 1	Alternative 2
TFP Growth Persistence (ρ_g)	0.50	0.30	0.25
Surprise TFP Persistence (ρ_s)	0.40	0.25	0.20
MEI Persistence (ρ_μ)	0.95	0.95	0.95
TFP Growth Shock SD (σ_g)	0.0025	0.0015	0.004
Surprise TFP Shock SD (σ_s)	0.006	0.006	0.007
MEI Shock SD (σ_μ)	0.004	0.006	0.0035

Notes: MEI is the marginal efficiency of investment.

Table 10: Data and model-implied moments from alternative larger-scale DSGE models

Moment	Data	Baseline	Alternative 1	Alternative 2
$SD(\tilde{a}_t)$	2.01	2.31	1.62	2.46
$SD(\Delta a_t)$	0.80	0.73	0.70	0.88
$SD(\tilde{y}_t)$	3.13	3.92	3.24	4.08
$SD(\tilde{\imath}_t)$	9.63	9.48	9.83	9.33
$AC(\tilde{a}_t)$	0.87	0.87	0.83	0.86
$AC(\Delta a_t)$	−0.09	0.01	−0.20	−0.12

Notes: A tilde denotes a detrended variable and Δ is a log change. In the data, a_t is Fernald utilization-adjusted TFP while in the model it is measured TFP (TFP_t^u).

Table 11: Forecast error variance decompositions for TFP in alternative larger-scale DSGE models

(a) Measured TFP ($\ln \text{TFP}_t^u$)

	Alternative 1			Alternative 2		
Horizon	News	Surprise	MEI	News	Surprise	MEI
4	10.2	59.8	30.1	43.0	50.4	6.5
8	14.4	53.4	32.1	53.4	40.3	6.2
20	9.4	6.3	84.3	62.2	8.2	29.5
40	13.4	1.3	85.3	73.4	1.4	25.3
80	20.9	0.7	78.4	82.6	0.5	16.9

(b) True TFP ($\ln a_t$)

	Alternative 1			Alternative 2		
Horizon	News	Surprise	MEI	News	Surprise	MEI
4	21.3	78.7	0.0	57.3	42.7	0.0
8	42.7	57.3	0.0	78.1	21.9	0.0
20	68.6	31.4	0.0	91.1	8.9	0.0
40	82.1	17.9	0.0	95.5	4.5	0.0
80	90.3	9.7	0.0	97.8	2.2	0.0

Notes: MEI is the marginal efficiency of investment.

Table 12: RMSE over 40 quarters based on alternative larger-scale DSGE models

(a) Alternative 1

Estimator	TFP Response	Output Response	Investment Response	Total
KS Max Share	8.6	12.6	49.6	70.8
BS Max Share	5.6	6.6	15.3	27.5
NAMS	8.2	11.0	41.4	60.6
Max Share News	3.2	2.2	6.4	11.9

(b) Alternative 2

Estimator	TFP Response	Output Response	Investment Response	Total
KS Max Share	10.2	10.7	19.4	40.3
BS Max Share	9.0	9.0	15.5	33.5
NAMS	9.9	11.2	21.9	42.9
Max Share News	6.5	2.6	7.2	16.3

Notes: VAR(4) with $T = 10{,}000$, where $\mathbf{y}_t = (\text{TFP}_t^u, y_t, i_t)$ for the TFP max share estimators and $\mathbf{y}_t = (z_{t+1}, \text{TFP}_t^u, y_t, i_t)$ for the max share news estimator.

REFERENCES

BARON, J. AND J. SCHMIDT (2019): "Technological Standardization, Endogenous Productivity and Transitory Dynamics," Manuscript, Northwestern University.

CASCALDI-GARCIA, D. AND M. VUKOTIĆ (2022): "Patent-Based News Shocks," *Review of Economics and Statistics*, 104, 51–66.

KOGAN, L., D. PAPANIKOLAOU, A. SERU, AND N. STOFFMAN (2017): "Technological Innovation, Resource Allocation, and Growth," *Quarterly Journal of Economics*, 132, 665–712.

KURMANN, A. AND E. SIMS (2021): "Revisions in Utilization-Adjusted TFP and Robust Identification of News Shocks," *Review of Economics and Statistics*, 103, 216–235.